Science and Technology Infusion Climate Bulletin
NOAA's National Weather Service
38th NOAA Annual Climate Diagnostics and Prediction Workshop
College Park, MD, 21-24 October 2013

Sea Ice in the NCEP Climate Forecast System Reanalysis

Xingren Wu[1, 2], and Robert Grumbine[1]

[1]*Environmental Modeling Center, NCEP/NWS/NOAA*

[2]*I.M. Systems Group, Inc., Rockville, MD*

ABSTRACT

The NCEP climate forecast system (CFS) reanalysis (CFSR) was recently completed using the NCEP coupled atmosphere-ocean-land surface-sea ice system. This paper describes the sea ice concentration data used and how sea ice concentration is assimilated in the CFSR. The near record minimum of Arctic sea ice is clearly shown in the CFSR output. Because of the realistic sea ice distribution, there have been many improvements in the CFSR compared to the previous NCEP/NCAR Reanalysis-1 and NCEP-DOE Reanalysis-2. For instance, the surface air temperature improved in the fall over the Arctic Ocean.

1. Introduction

Sea ice is known to play a significant role in the global climate system. Realistic representation of sea ice is essential for good performance of atmospheric and oceanic data assimilation models over the polar regions in the CFSR. Global climate modeling studies show that sea ice concentration has a strong impact on the climate over the Antarctic regions (*e.g.*, Simmonds and Budd 1991; Simmonds and Wu 1993). Recent studies (*e.g.*, Overland and Wang 2010; Screen and Simmonds 2010; Liu *et al.* 2012) demonstrate that the declining Arctic sea ice has a significant impact on the atmospheric circulation, surface latent heat flux and winter snowfall. We note that, there was no sea ice concentration in the previous NCEP reanalysis, the NCEP/NCAR Reanalysis-1 (R1) (Kalnay *et al.* 1996) and NCEP-DOE Reanalysis-2 (R2) (Kanamitsu *et al.* 2002), although sea ice concentration data from analysis were used to present the sea ice coverage in R1 and R2 with 55% cutoff (*i.e.* when sea ice concentration is greater than 55% it is considered as 100% sea ice coverage). The new CFSR at NCEP (Saha *et al.* 2010) allows us to add sea ice concentration from analysis into the reanalysis system, which leads to more realistic interactions between sea ice and atmosphere in the polar regions. This paper describes the sea ice data used in the CFSR, how sea ice concentration is assimilated, and discusses the implications for improvement in the products of the CFSR.

2. The sea ice concentration analysis

The sea ice analysis produces a global record of sea ice concentration for the CFSR for all points that may freeze anywhere in the globe. This is done daily on a grid of 0.5 degree latitude-longitude resolution throughout the period of the CFSR. When there are discontinuities in the production of the data set, newer data sets and newer methods are used.

From 1979 to 1996, the sea ice concentrations for most of the globe are regridded from Cavalieri *et al.* (1996, updated 2007) (GSFC Ice), except for (i) possibly ice-covered regions that lie outside that grid, (ii) large Canadian lakes, (iii) the Great Lakes, and (iv) sea surface temperature-based filtering of erroneous ice in the analysis. For the Great Lakes, the data used are Assel *et al.* (2002) from 1979 through the end of the data set in Spring, 2002, and passive microwave thereafter. Those grids are available 1-3 times per week throughout the period they are available. Concentrations were linearly interpolated between the observation dates, and those interpolated values are used here, averaged on to the target 0.5 degree grid from the native 2.55 km Mercator projection. For large lakes in Canada, the Canadian Ice Service (CIS, personal

Correspondence to: Xingren Wu, Environmental Modeling Center, NCEP/NWS/NOAA, 5830 University Research Court, College Park, MD 20740-3818; Email: Xingren.Wu@noaa.gov

communication) analyses were used for all lakes which were analyzed from November 1995 through October 29, 2007 (initially 34, in November, 1995, increasing to 137 by October, 2007). From October 30, 2007 onwards, the concentrations are the operational NCEP passive microwave sea ice concentration analyses.

There are regions which may freeze but lie outside the domain analyzed in GSFC Ice. These large water bodies were analyzed by proxy over 1979-1996, as was done for portions of the North American Regional Reanalysis (Mesinger *et al.* 2006). Proxies were generated anew for the CFSR as the domain is much larger, and more data are available. During the period 1 January 1997 - 30 June 2006 when both NCEP ice and GSFC ice were available, the NCEP ice analysis was used to identify points (one by one) which lay inside the GSFC ice domain and which had high correlation to concentrations analyzed for points outside the GSFC ice domain - but still inside the NCEP domain. This includes large lakes such as Lake Ladoga, Lake Onega, and the Caspian Sea. Due to changes in sea surface temperature (SST) sources for filtering sea ice concentration analyses, some regions such as the Aral Sea, Lakes Balkhash, and Hulun Nur could not be consistently analyzed and were assigned zero ice concentration. Some lakes were assigned land flags in the CFSR when they could not be observed strictly by modern passive microwave due to land contamination issues and the lack of available data; these lakes include Lake Athabasca, Lake of the Woods, Lake Nipigon (outside the period of CIS data), Iliamna Lake, and Lake Vanern.

From January 1997-February 2000, the global ice concentration analysis was the NCEP operational ice analysis (Grumbine 1996) (outside the Great Lakes and Canadian Lakes). From 1 March 2000 to 29 October 2007, the sea ice analysis is the newer NCEP sea ice analysis system applied to archived passive microwave data for DMSP F-13, F-14, and F-15. The old NCEP system was based on the NASA Team1 algorithm (Cavalieri 1992) as was the GSFC ice. The newer system is based on the Team2 algorithm (Markus and Cavalieri 2000). In the newer NCEP system, the sea ice concentration for each day is computed by regression of the Stokes-like parameter $(T85V^2 - T85H^2)^{0.5}$ (where T85V is the 85 GHz brightness temperature at vertical polarization, and T85H is likewise for the horizontal polarization) against the Team2-derived concentration - for those points that are greater than 100 km from land, and are poleward of 60 degrees latitude. The regression provides an unbiased estimator, and, due to the small footprint of the 85 GHz channel, a higher resolution estimate, permitting analysis closer to the coast and inside smaller lakes than would otherwise be possible with the pure Team2 algorithm. This operational system used the SSMI (Special Sensor Microwave/Imager) instruments on DMSP F-13, F-14, and F-15 while those were all available. F-14 stopped providing data in October 2008. F-15 suffered progressively more severe corruption of the 22 GHz channel in late 2008 and was removed from NCEP sea ice production 5 March, 2009. AMSR-E was added to the operational sea ice system on 13 May 2009, using the AMSR-E Team2 algorithm with January, 2009 tie points as described in Markus and Cavalieri (2009). That date was concurrent with a data flow outage from AMSR-E and data corruption in F-13. This simultaneous failure degraded the quality of the sea ice analysis in May 2009. Sea ice data were reprocessed for the CFSR using F-13 and AMSR-E from February to April. The passive microwave weather filters are imperfect, meaning that ice concentrations can be reported from the microwave for reasons other than ice being on the surface, so that an SST filter is also used (Grumbine 1996). The sea ice concentrations were in general produced before the SST analyses used for the CFSR. Therefore, an a posteriori filter was used for retrospective analyses through 29 October 2007 (Grumbine 2009). The usual SST filtering was also done using AVHRR-Only analysis (Reynolds *et al.* 2007) for 4 January 1985-10 February 2000. The real-time global (RTG) low resolution analysis (Thiebaux *et al.* 2003) was used 11 Feb 2001 through 29 October 2007 and RTG high resolution analysis (Gemmill *et al.* 2007) thereafter.

3. The coupled model

The model used for the CFSR is the NCEP coupled atmosphere-ocean-land surface-sea ice model. The atmospheric model is based on the previous NCEP operational global forecast system (GFS) model with improvements including new radiation and physics (Saha *et al.* 2010). The horizontal resolution is T382 with 64 hybrid vertical layers. The ocean model is from GFDL Modular Ocean Model version 4p0d (MOM4, Griffies *et al.* 2004), with 40 vertical layers. The zonal resolution of MOM4 is $1/2^o$. The meridional resolution is $1/4^o$ between 10^oS and 10^oN, gradually increasing through the tropics becoming $1/2^o$ poleward of 30^oS and 30^oN. The ocean model uses a tripolar grid north of 65^oN. The land surface model is the NOAH land surface

model (Ek *et al.* 2003), which is imbedded in the GFS. The sea ice model is described below. Full details of the model description for the atmosphere, ocean, and land surface can be found in Saha *et al.* (2010).

4. The sea ice model

The sea ice model is from GFDL Sea Ice Simulator with slight modifications. Similar to the ocean model, sea ice model components use a tripolar grid north of 65°N, *i.e.*, a grid that has "poles" located in the land masses of northern Canada and northern Russia, in addition to the normal South Pole. There are three layers for the sea ice model, including two equal layers of sea ice and one (optional) layer of snow with five categories of sea ice thickness (0-0.1, 0.1-0.3, 0.3-0.7, 0.7-1.1, and the category greater than 1.1 m). The snow has no heat capacity, the upper ice layer has sensible and latent heat capacity (*i.e.* a variable temperature/ salinity dependent), and the lower ice layer has only sensible (fixed) heat capacity. The base of ice is fixed at the (salinity dependent) seawater freezing temperature. Sea ice dynamics is based on Hunke and Dukowicz (1997) using the elastic-viscous-plastic technique to calculate ice internal stress. The ice strength follows that of Hibler (1979). Ice thermodynamics is based on Winton (2000). It is possible for ice to be transferred conservatively between the snow layer and the two ice layers when there is snowfall, evaporation, freezing, or melting. When sea ice forms over the ocean, it releases latent heat and salt to the ocean. Details can be found in Griffies *et al.* (2004).

5. The assimilation of sea ice concentration in the CFSR

Due to the lack of observations of sea ice thickness and motion covering the CFSR period starting 1979, a sea ice merging scheme is used in the CFSR to add sea ice concentration into the system. The 6-hour model guess field and the analyzed sea ice concentration are used to produce a

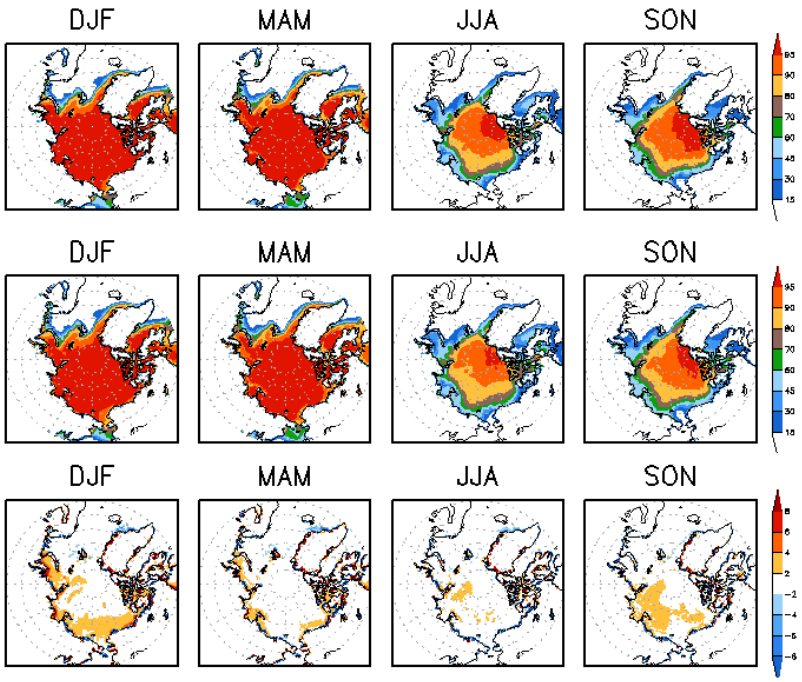

Fig. 1 Sea ice concentration (%) in the Arctic averaged from 1979 to 2010 for December-January-February (DJF), March-April-May (MAM), June-July-August (JJA) and September-October-November (SON) from the CFSR (top), the analysis (middle) and the difference between the CFSR and the analysis (bottom). The contours are 15/30/45/60/70/80/90/95 for the sea ice concentration and -8/-6/-4/-2/2/4/6/8 for the difference.

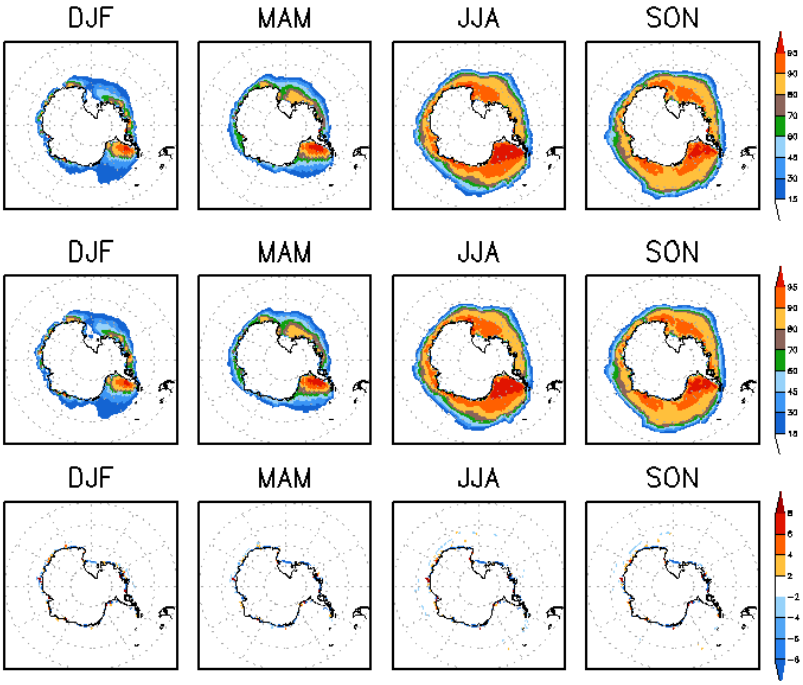

Fig. 2 As in Fig. 1 but for the Antarctic.

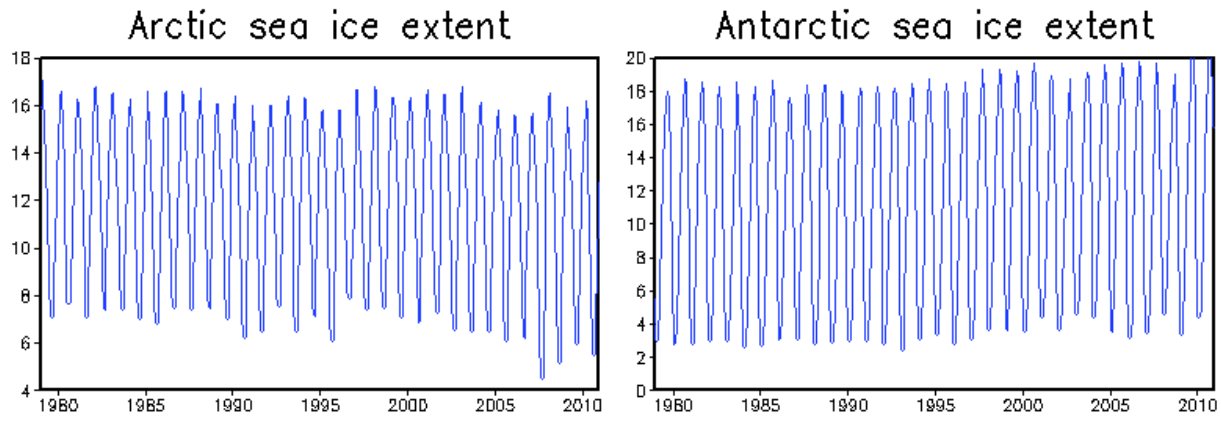

Fig. 3 Monthly mean sea ice extent (10^6 km^2) for the Arctic (left) and Antarctic (right) from the CFSR.

new initial condition. During the merging process, a quality control is applied to prevent the failure when there is a feedback between the ice analysis and the SST analysis. This is done on the sea ice model grid after the interpolation (regridding) is performed for SST and sea ice concentration. When the SST from the analysis is warmer than 275.3 K, or the sea ice concentration from the analysis is less than 15%, no sea ice is allowed to exist, so sea ice is removed from the CFSR initial condition. When the sea ice concentration from the analysis is greater than (or equal to) 15% and the SST is not warmer than 275.3 K, the CFSR initial sea ice concentration is reset to the analyzed value. If the model guess contains more sea ice, thin ice is removed first before thicker ice. In summer, the melt pond effect on ice albedo is considered1, which is done for the Arctic sea ice cover north of 70°N only. When there are serious problems for sea ice concentration data from analysis, we only use model predictions. This happens for May 1-13, 2009.

6. Sea ice in the CFSR

Because sea ice concentration has been "assimilated", there is no doubt that the ice field is very close to the observations for sea ice concentration and ice coverage. Figure 1 shows the sea ice concentration averaged from 1979-2010 in the CFSR for December-January-February (DJF), March-April-May (MAM), June-July-August (JJA), and September-October-November (SON) for the Arctic, the corresponding analysis, and the difference between the CFSR and the analysis. It can be seen that the difference is very small and mostly along the coast. The Antarctic sea ice concentration for each season from the CFSR and the analysis is shown in Figure 2 with the difference given. The difference over the Antarctic is even smaller and almost negligible.

The Arctic region sea ice reaches its maximum coverage in late February or early March and minimum

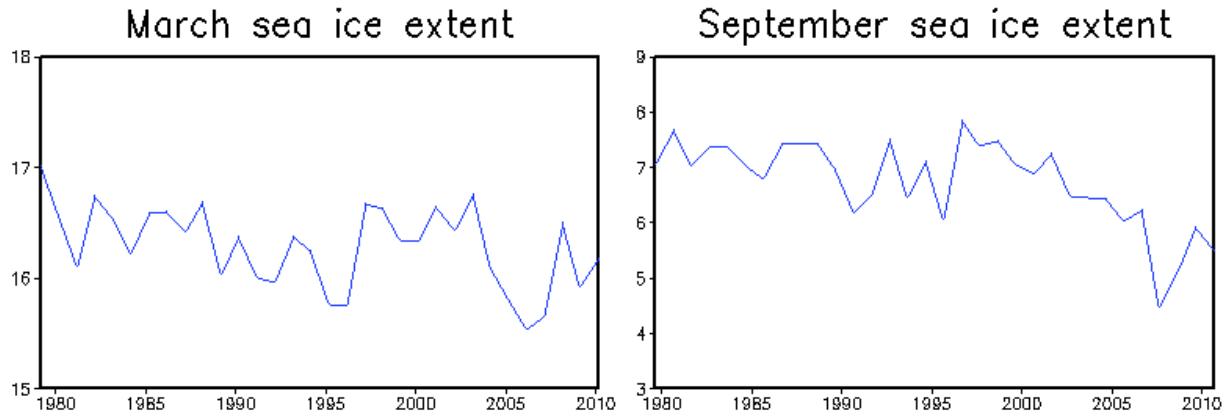

Fig. 4 Arctic sea ice extent (106 km^2) from the CFSR in March (left) and September (right).

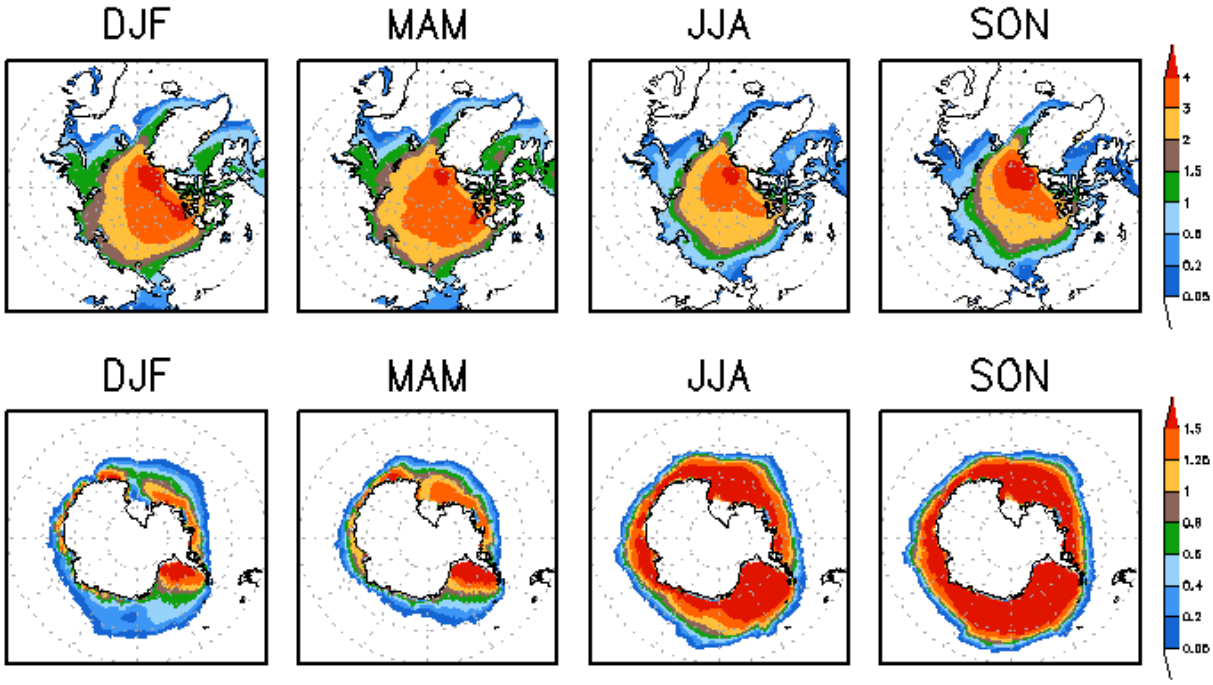

Fig. 5 Sea ice thickness (m) in the Arctic (top) and Antarctic (bottom) averaged from 1979 to 2010 for DJF, MAM, JJA and SON from the CFSR. The contours are 0.05/0.2/0.5/1/1.5/2/3/4 for the Arctic and 0.05/0.2/0.4/0.6/0.8/1/1.25/1.5 for the Antarctic.

coverage in September. From November to June, sea ice covers 90% of the Arctic Ocean, where the open water region is very small. The Antarctic sea ice reaches its maximum coverage in September and minimum coverage in February. Much larger seasonal variation of sea ice exists in the Antarctic than in the Arctic. Sea ice extent, which is defined as the total area with sea ice present (including open water) for which each grid cell has at least 15% sea ice, is shown in Figure 3. It can be seen that the maximum sea ice extent is about three times the minimum sea ice extent for the Arctic, but it is about nine times for the Antarctic. Large reductions in sea ice are obvious in the CFSR for both summers of 2007 and 2008 over the Arctic. Inter-annual variability for the total sea ice extent is relatively small for both hemispheres but regional inter-annual variation for the marginal sea ice zone is very large (not shown). The overall trend over the 32-year period is slightly positive for the Antarctic and negative for the Arctic, which is consistent with previous studies (*e.g.*, Comiso and Nishio 2008; Parkinson 2006). The March and September Arctic sea ice extent is shown in Figure 4. This is comparable to that from Stroeve *et al.* (2007), in particular for the sea ice trend for September. The plots in Stroeve stopped at 2006, whereas our CFSR data includes 2007-2010.

The seasonal sea ice thickness for the 32-year mean is shown in Figure 5. Sea ice is much thicker over the Arctic than over the Antarctic. The averaged sea ice thickness in the CFSR is reasonable in the Arctic for the first 20 years but it is too thick for the last decade; it might also be too thick in the Antarctic

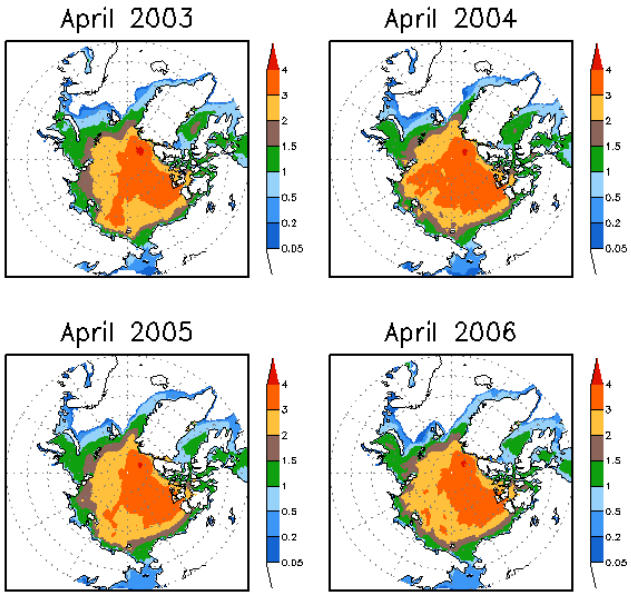

Fig. 6 Sea ice thickness (m) for April from 2003 to 2006 in the Arctic from the CFSR. The contours are 0.05/0.2/0.5/1/1.5/2/3/4.

as the observed Antarctic sea ice is mostly less than 1 m (*e.g.*, Wadams *et al.* 1987; Worby *et al.* 1994). Maslanik *et al.* (2007) showed a large interannual variation of Arctic spring sea ice thickness between 2003 and 2006. The sea ice thickness for April from the CFSR is shown here (Fig. 6) for 2003-2006. The interannual variation from the CFSR is not as large as the observations shown in Maslanik *et al.* (2007). The sea ice thickness errors can result from deficiencies in any component of the coupled atmosphere-ocean-land surface-sea ice model and their interactions. One example is the downward shortwave radiation. When the CFSR model is used to do seasonal forecast there is a cold SST bias in the Tropics, leading to an El Nino/Southern Oscillation variability that is too weak (Saha *et al.* 2014). Nevertheless, the CFSR is able to simulate the large reduction in sea ice over the past 20 years. Figure 7 shows the sea ice concentration and thickness for September of 1987 and 2007 for the Arctic. Record minimum Arctic sea ice cover was observed in September 2007 (*e.g.* Comiso *et al.* 2008), which was broken again in 2012. The sea ice thickness in the CFSR also shows a large reduction from 1987 to 2007.

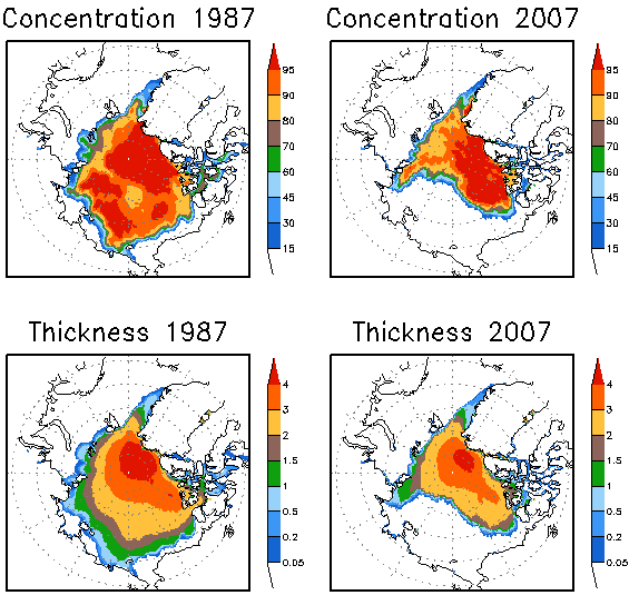

Fig. 7 Sea ice concentration (%) and thickness (m) for September 1987 and 2007 from the CFSR for the Arctic.

8. Summary

We have described the sea ice data used in the NCEP CFSR and how sea ice is assimilated. This is the first reanalysis at NCEP where sea ice concentration is assimilated into the reanalysis system. Because of the realistic sea ice distribution and other improvements in the CFSR, it is expected that the coupled reanalysis has been improved in many aspects over the polar regions compared with the previous R1 and R2 (*e.g.* Wang *et al.* 2010). Figure 8 shows the difference in surface air temperature (SAR) among CFSR and R1, R2, and ERA40 (ECMWF Re-Analysis System, Uppala *et al.*, 2005) for the Arctic in September. It can be seen that, due to the lack of open water in the sea ice zone in R1 and R2, the surface air temperatures from R1 and R2 are colder than CFSR in September, but there is good agreement between CFSR and ERA40. Large and Yeager (2004) showed that the mean SAR in R1 for September during 1979-1998 north of 70°N is about 1.7°C colder than observations. For our case during 1979-2009, CFSR is 1.8°C warmer than R1 over the same region, 1.3°C warmer than R2, and 0.2°C warmer than ERA40. This cold bias in R1 for September has been completely removed in the CFSR.

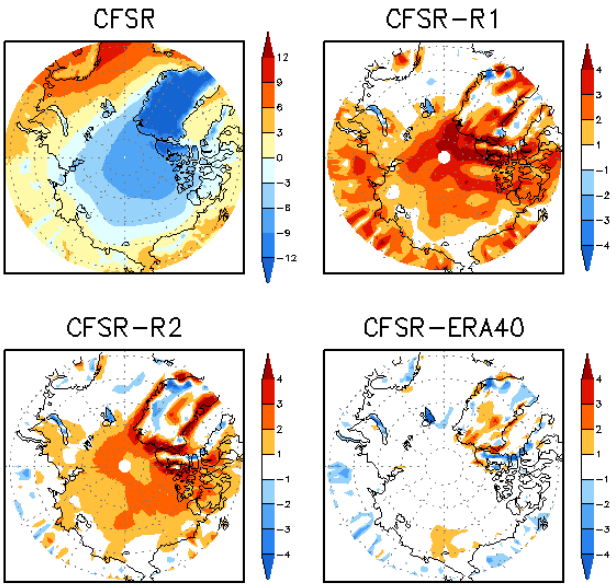

Fig. 8 Mean surface air (2m) temperature (°C) averaged 1979-2009 for September from the CFSR for the Arctic (top left), and the difference among CFSR and R1, R2 and ERA40. The surface air temperatures from R1 and R2 are also averaged over 1979-2009, but averaged over 1979-2001 for ERA40.

Acknowledgements. We acknowledge all members of the CFSR team at NCEP.

References

Assel, R. A., David C. Norton, and K. C. Cronk, 2002: A Great Lakes ice cover digital data set for winters 1973-2000, *NOAA Technical Memorandum GLERL-121*, 46 pp.

Cavalieri, D. J., 1992: Sea ice algorithm. NASA sea ice validation program for the Defense Meteorological Satellite Program Special Sensor Microwave Imager: Final Report. *NASA Technical Memorandum 104559*, 25-31.

Cavalieri, D. J., C. L. Parkinson, P. Gloersen, and H. J. Zwally, 1996: Sea ice concentrations from Nimbus-7 SMMR and DMSP SSM/I-SSMIS passive microwave data, 1978-1996. Boulder, Colorado USA, NASA DAAC at the National Snow and Ice Data Center. Digital Media. Updated 2007.

Comiso, J. C., and F. Nishio, 2008: Trends in the sea ice cover using enhanced and compatible AMSR-E SSM/I, and SMMR data. *J. Geophys. Res.*, **113**, C02S07, doi:10.1029/2007JC004257.

Comiso, J. C., C. L. Parkinson, R. Gersten, and L. Stock, 2008: Accelerated decline in the Arctic sea ice cover. *Geophys. Res. Lett.*, **35**, L01703, doi:10.1029/2007GL031972.

Ek, M. B., K. E. Mitchell, Y. Lin, E. Rogers, P. Grunmann, V. Koren, G. Gayno, and J. D. Tarplay, 2003: Implementation of the Noah land-use model advances in the NCEP operational mesoscale Eta model. *J. Geophys. Res.*, **108**, 8851, doi:10.1029/2002JD003296.

Gemmill, W., B. Katz, and X. Li, 2007: Daily real-time, global sea surface temperature, a high-resolution analysis: RTG_SST_RH. *NOAA/NWS/NCEP/MMAB Technical Notes 260*, 39 pp.

Griffies, S. M., M. J. Harrison, R. C. Pacanowski, and A. Rosati, 2004: A technical guide to MOM4. *GFDL Ocean Group Technical Report No. 5*, NOAA/Geophysical Fluid Dynamics Laboratory, Available online at http://www.gfdl.noaa.gov/~fms.

Grumbine, R. W., 1996: Automated passive microwave sea ice concentration analysis at NCEP. *NOAA/NWS/NCEP/OMB Technical Note 120*, 13 pp.

Grumbine, R. W., 2009: A posteriori filtering of sea ice concentration analyses. *NOAA/NWS/NCEP/MMAB Techical Notes 282*, 7 pp.

Hibler, W. D. III, 1979: A dynamic thermodynamic sea ice model, *J. Phys. Oceanogr.*, **9**, 815-846.

Hunke, E. C., and J. K. Dukowicz, 1997: An elastic-viscous-plastic model for sea ice dynamics. *J. Phys. Oceanogr.*, **27**, 1849-1867.

Kalnay, E., M. Kanamitsu, R. Kistler, W. Collins, D. Deaven, and Co-authors, 1996: The NCEP/NCAR 40-Year Reanalysis Project. *Bull. Amer. Meteor. Soc.*, **77**, 437-471.

Kanamitsu, M., W. Ebisuzaki, J. Woollen, S. K. Yang, J. J. Hnilo, M. Fiorino, and G. L. Potter, 2002: NCEP-DOE AMIP-II Reanalysis (R-2). *Bull. Amer. Meteor. Soc.*, **83**, 1631-1643.

Large, W. G., and S. G. Yeager, 2004: Diurnal to decadal global forcing for ocean and sea-ice models: The data sets and flux climatologies. *NCAR Technical Note, NCAR/TN-460+STR*, 105pp.

Liu, J., J. A. Curry., H. Wang, M. Song, and R. M.Horton, 2012: Impact of declining Arctic sea ice on winter snowfall. *Proceeding of the National Academy of Sciences of the United States of America*, **109**, 4074-4079.

Markus, T., and D. J. Cavalieri, 2000: An enhancement of the NASA team sea ice algorithm. *IEEE Transactions on Geoscience and Remote Sensing*, **38**, 1387-1398.

Markus, T., and D. J. Cavalieri, 2009: The AMSR-E NT2 sea ice concentration algorithm: Its basis and implementation. *Journal of the Remote Sensing Society of Japan*, **29**, 216-225.

Maslanik, J. A., C. Fowler, J. Stroeve, S. Drobot, J. Zwally, D. Yi, and W. Emery, 2007: A younger, thinner Arctic ice cover: Increased potential for rapid, extensive sea-ice loss. *Geophys. Res. Lett.*, **34**, L24501, doi:10.1029/2007GL032043.

Mesinger, F., G. DiMego, E. Kalnay, K. Mitchell, P. C. Shafran, W. Ebisuzaki, D. Jović, J. Woollen, E. Rogers, E. H. Berbery, M. B. Ek, Y. Fan, R. Grumbine, W. Higgins, H. Li, Y. Lin, G. Manikin, D. Parrish,

and W. Shi, 2006: North American Regional Reanalysis. *Bull. Amer. Meteor. Soc.*, **87**, 343–360, doi: 10.1175/BAMS-87-3-343.

Overland, J. E., and M. Wang, 2010: Large-scale atmospheric circulation changes associated with the recent loss of Arctic sea ice. *Tellus*, **62A**, 1-9.

Parkinson, C. L., 2006: Earth's Cryosphere: Current state and recent changes. *Review of Environment and Resources*, **31**, 33-60.

Reynolds, R. W., T. M. Smith, C. Liu, D. B. Chelton, K. S. Casey, and M. G. Schlax, 2007: Daily high-resolution-blended analyses for sea surface temperature. *J. Climate*, **20**, 5473-5496.

Saha, S., S. Moorthi, H.-L. Pan, X. Wu, J. Wang, S. Nadiga, P. Tripp, and Co-authors, 2010: The NCEP Climate Forecast System Reanalysis. *Bull. Amer. Meteor. Soc.*, **91**, 1015-1057.

Saha, S., S. Moorthi, X. Wu, J. Wang, S. Nadiga, P. Tripp, and Co-authors, 2014: The NCEP Climate Forecast System version 2. *J. Climate*, (in press).

Screen, J. A., and I. Simmonds, 2010: The central role of diminished sea ice in recent Arctic temperature amplification. *Nature*, **464**, 1334-1337, doi:10.1038/nature09051.

Simmonds, I., and W. F. Budd, 1991: Sensitivity of the southern hemisphere circulation to leads in the Antarctic pack ice. *Q. J. R. Meteorol. Soc.*, **117**, 1003-1024.

Simmonds, I., and X. Wu, 1993: Cyclone behaviour response to changes in winter southern hemisphere sea-ice zone. *Q. J. R. Meteorol. Soc.*, **119**, 1121-1148.

Stroeve, J., M. M. Holland, W. Meier, T. Scambos, and M. Serreze, 2007: Arctic sea ice decline: Faster than forecast. *Geophys. Res. Lett.*, **34**, L09501, doi:10.1029/2007GL029703.

Thiébaux, J., E. Rogers, W. Wang, and B. Katz, 2003: A new high-resolution blended real-time global sea surface temperature analysis. *Bull. Amer. Meteor. Soc.*, **84**, 645–656, doi: 10.1175/BAMS-84-5-645.

Uppala, S. M., and Co-authors, 2005: The ERA-40 re-analysis. *Q. J. R. Meteorol. Soc.*, **131**, 2961-3012.

Wadhams, P., M. A. Lange, and S. F. Ackley, 1987: The ice thickness distribution across the Atlantic sector of the Antarctic Ocean in midwinter. *J. Geophys. Res.*, **92**, 14535-14552.

Wang, W., P. Xie, S.-H. Yoo, Y. Xue, A. Kumar, and X. Wu, 2010: An assessment of the surface climate in the NCEP Climate Forecast System Reanalysis. *Clim. Dyn.*, **37**, 1601-1620.

Winton, M., 2000: A reformulated three-layer sea ice model. *J. Atmos. Oceanic Technol.*, **17**, 525-531.

Worby, A. P., W. F. Weeks, M. O. Jeffries, K. Morris, and R. Jana, 1994: Late winter-sea-ice-thickness and snow-thickness distribution in the Bellingshausen and Amundsen Seas. *Antarctic Journal of the United States*, **29**, 13-15.